Pak. J. Bot., 57(5): DOI: http://dx.doi.org/10.30848/PJB2025-5(9)

THE NOVEL ANTIFUNGI OF ROSE MYRTLE FRUIT MICROWARE EXTRACT (*RHODOMYRTUS TOMENTOSA*) *IN VITRO* AND *IN SILICO* DOCKING

NGUYEN VAN HUE[1], TRAN NGUYEN MINH AN[2*] AND LE VAN TAN[2*]

[1]University of Agriculture and Forestry, Hue University, 52000, Vietnam
[2]Faculty of Chemical Engineering, Industrial University of Ho Chi Minh City, Vietnam, 12 Nguyen Van Bao Street, Go Vap District, Ho Chi Minh City Vietnam, 727010
**Corresponding author's email: trannguyenminhan@iuh.edu.vn; tanlevan@iuh.edu.vn*

Abstract

Myrtle fruit (*Rhodomyrtus tomentosa*) contains a large amount of phenolic compounds, which have been shown to have high biological activity with antioxidant, anti-cancer, and anti-obesity properties. The myrtle extract was evaluated for its antioxidant and antibacterial properties. The antioxidant activities of myrtle fruit extract were analyzed DPPH radical inhibition assay. The myrtle extract had an IC_{50} of 233.98 $g.mL^{-1}$ and the antioxidant activity that was weaker than that of vitamin C. The gas chromatography–mass spectrometry (GC-MS) method with an HP5-MS column was used to analyze some biologically active compounds in myrtle extract. The myrtle extract contained 19 compounds, of which only two compounds were identified. It was noticeable that 2,3-dihydro-3,5-dihydroxy-6-methyl-4H-pyran-4-one was present in myrtlee extract, a flavonoid compound that played an important role in cancer prevention, cardiovascular disease prevention, and liver function protection. The novel anti fungi activity of rose myrtle fruit extract agianst *Alternaria alternata* apple pathotype at concentrations of MIC of 25 $mg.mL^{-1}$ showed excellent activites. *In silico* docking model, pose 698, one the best docking pose among 1000 docking conformations of compound 12 docked well to 4AUD:PDB protein, and compound 12 or pose 505 inhibited well to 2VF5: PDB enzyme to explain the general mechanism about synthesis inhibition of bacteria or fungi cell wall in silico docking model of the best conformation of compound 12 to 2VF5 enzyme that proved why compound 12 showed good activity *In vitro*. Fruit extraction of rose myrtle was extracted using microwave equipment. The components of rose myrtle fruit extraction depend on the solvent polarity, ratio of solid and solvent, microware power, and time in microware treatment.

Key words: Antioxidant, Antifungal, Microware extract, Rose myrtle, *Rhodomyrtus tomentosa*, *In silico* docking

Introduction

Rose myrtle (*Rhodomyrtus tomentosa*), known by various names such as Downy myrtle, Hill gooseberry, and Ceylon Hill cherry, belongs to the Myrtaceae family (Lim, 2012). Its distribution in Vietnam spans from the northern to the southern regions, where it thrives in scattered or concentrated growth on shrub hills, effectively mitigating erosion in midlands and low mountains. *Rhodomyrtus tomentosa*, a resilient wood species, flourishes in environments with minimal soil requirements and shows remarkable resistance against pests and diseases. Notably, China, Taiwan, the Philippines, Malaysia, Indonesia, and Vietnam harbor populations of this plant. Historical accounts and artistic depictions suggest that *R. tomentosa* held significant medicinal importance in the lives of ancient cultures, offering remedies for various ailments as documented in literature and artwork. Its pharmacological profile encompasses a wide spectrum of effects, including treatment for colic, diarrhea, wounds, heartburn, abscesses, gynecopathy, and pain. In the practice of traditional Chinese medicine, R. tomentosa was historically utilized to address urinary tract infections. This plant has revealed the presence of 42 compounds whose structures have been elucidated. These compounds include phloroglucinol, flavonoids, terpenoids, anthracene glycosides, tannins, others. Among these compounds, rhodomyrtone, an acylphloroglucinol, has shown effectiveness against a broad array of Gram-positive bacteria, displaying antimicrobial and anti-infective properties. Its diverse biological activities include antibacterial, antifungal, antimalarial, osteogenic, antioxidant, and anti-inflammatory effects. Researchers have extensively investigated *R. tomentosa* as an antimicrobial agent (Hamid *et al.*, 2016). The abundant chemical diversity found in this plant presents opportunities for developing new drug candidates, whether in the form of pure compounds or standardized extracts derived from natural products (Cos *et al*., 2006). The utilization of herbal medicines in Asia reflects a long history of human engagement with nature. Various traditional medicinal plants yield a wide range of substances capable of treating chronic and infectious diseases (Sasidharan *et al*., 2011). Myrtle fruit contains large amounts of phenolic compounds, especially ellagitannins, stilbenes, anthocyanins, flavonols, and phenolic acids (Lai *et al.*, 2013). Among them is the notable component piceatannol, a potent biologically active stilbene with antioxidant (Zdenka *et al.*, 2006), anti-cancer (Kita *et al.*, 2012), and anti-obesity properties (Kwon *et al.*, 2012). Furthermore, piceatannol serves as the primary component, constituting up to 19% of the total phenolic compounds identified in the fruit. According to Lai *et al*., (2013), the content of piceatannol in myrtle fruit surpasses that is found in grapes by a substantial margin, with levels ranging from 1000 to 2000 times higher. In addition, recent studies have found that the leaves and stems of myrtle also contain some antibiotics (rhodomyrtone) that are effective against some bacteria that cause food poisoning, such as: Streptococcus pyogenes (Limsuwan & Voravuthikunchai, 2008), *Escherichia coli* (Dachriyanus *et al.*, 2002), *Staphylococcus aureus* (Saising *et al.*, 2008). Currently, drug design using computer tools is the current trend and autodock, MOE, Autodock vina, Glide Schrodinger, and Hex software are interesting solutions to predict SAR (Morris *et al.*, 2009; Huey *et al.*, 2012; Ravindranath *et al.*, 2015). To explain the bioactivities *In silico*, many articles are used autodock to solve

this problems (Thuy *et al*., 2020; Nguyen *et al.*, 2022; Mai *et al.*, 2022; Vo *et al.*, 2022; Nguyen *et al.*, 2022; Pham *et al.*, 2022; Tri *et al.*, 2023; Duy *et al.*, 2023; Trinh *et al.*, 2023). The validations of docking model needs to be checked if the conformation change of one ligand attached to enzyme or protein is validated via RMSD value of pair of pose (Sargsyan *et al.*, 2017; Bell *et al.*, 2019; Agrawal *et al.*, 2019). The complex of the best docking pose among docking poses and enzyme have been selected to calculate in dynamic environment or real environment (temperature, pressure, and concentration of sodium chloride) that determines stable likeness drug by simulation time course in range 100 ns (Van-Der-Spoel *et al.*, 2005; Shaw, 2011; Abraham *et al.*, 2015; Ash & Fourches, 2017; Ece, 2023; Tri *et al.*, 2023). Until now, the utilization of the rose myrtle plant in Vietnam's food sectors remained significantly restricted. This limitation stems from the inadequate dissemination of information regarding the plant's cultivation techniques and advantages. Consequently, products derived from the rose myrtle have not garnered sufficient attention. Despite its potential benefits, particularly its fruit, the rose myrtle plant is largely unrecognized, often regarded as a weed. Consequently, it persists as a troublesome pest plant that proves challenging to manage. Hence, our research aims to delve into the chemical composition and assess the biological potential of rose myrtle fruit cultivated in central Vietnam.

Material and Methods

Materials: Ripe myrtle fruit (*Rhodomyrtus tomentosa*) was purchased in Hung Phuc commune, Hung Nguyen district, Nghe An province, Vietnam. Raw materials, after being collected, were sorted, washed, and dried (by Labtech LDO-080N Dryer, Korea) at 60^{o}C to the required moisture content (8–10%), then finely ground and stored at -35^{o}C until analysis.

Extract process: The ground Ripe myrtle fruit powder was extracted using ethanol (50%, 60%, 70%, 80%, 90%), with the following ingredient ratios: solvent (1:10, 10:20, 1:30, 1:40, 1:50) (g.mL^{-1}), microwave at 320W, 480W, 640W, 800W and treatment time of 3, 4, 5, 6 minutes (MDS-6G Multiflux Microwave Digestion Extraction System).The extract was then filtered and centrifuged at 5000 rpm for 10 minutes (Centrifuge machine LC-05A, China). The obtained solution was evaporated under vacuum at 50^{o}C to remove the solvent (Rotary Evaporator N-1300V-WB, Japan), before obtaining concentrated extract from rose myrtle fruit.

Qualitative analysis of total phenolic content: The total phenolic content (TPC) was determined by the Folin-Ciocalteu, following the method outlined by Li *et al*., (2007). In summary, 0.50 mL of the diluted sample was mixed with 2.5 mL of Folin–Ciocalteu reagent diluted at a ratio of 1:10. After 4 minutes, 2 mL of saturated sodium carbonate solution (approximately 75 g/L) was added. Following a 2-hour incubation at room temperature, the absorbance of the reaction mixture was measured at 760 nm. Gallic acid served as the reference standard, and the results were expressed as milligrams of gallic acid equivalent (mg GAE) per gram of dry weight of the plant material. Folin–Ciocalteu's phenol reagent and gallic acid were purchased from Sigma–Aldrich (St. Louis, MO).

Qualitative analysis of total phenolic content: The total flavonoids content (TFC) were assessed using a colorimetric method (Chang *et al.*, 2002). This method relies on the principle that flavonoids create a yellow complex when combined with $AlCl_3$ solution. The intensity of the color is directly proportional to the flavonoid content, which is measured at a wavelength of 415 nm. Catechin served as the standard in this analysis. Catechin were purchased from Sigma–Aldrich (St. Louis, MO).

Antioxidant activity: The antioxidant activities of rose myrtle fruit extract were analyzed following the 1,1-diphenyl-2-picrylhydrazyl (DPPH) radical inhibition assay (Plank *et al.*, 2012). The sample was diluted to the appropriate concentration, 100 µL of the diluted sample, into a test tube. The control sample replaced ethanol (99.6%). Then, added a tube of 100 µL DPPH solution to a test tube and left it in the dark for 30 min. The absorbance at 517 nm of the sample mixture and DPPH after 30 minutes of reaction in the dark was measured. Each sample was replicated three times, and the average value was taken. The% DPPH free radical scavenging activity was calculated from the measured OD of 517 nm using the following formula:

$$\%\ \text{The DPPH radical scavenging activity} = \frac{CD_C - OD_m}{OD_C} \times 100$$

In which: ODc optical density value of the blank; ODm: optical density value of the test specimen

Microbiological analysis: Antimicrobial susceptibility was assessed by the Kirby-Bauer disc diffusion method to determine the resistance of *Escherichia coli (E. coli)*, *Salmonella* sp., to various antimicrobial compounds (Hudzicki, 2009). The concentrations tested were 500, 250, 125, 62.5 mg.mL^{-1} and distilled water. Samples were impregnated on paper at different concentrations, then placed on nutrient agar plates inoculated with *E. coli*, *Salmonella* sp. The antibacterial ability of myrtle extraction was determined by measuring the diameter of the sterile ring around the sample impregnated paper.

Antifungal activity: The antifungal efficacy of rose myrtle fruit extract was evaluated using the well diffusion method against three strains: (AA: *Alternaria alternata* apple pathotype, AC: *Alternaria citri*, AAJ: *Alternaria alternata* Japanese pear pathotype), sourced from the Japanese Type Culture Collection (National Ehime University, Japan). Before commencing the antifungal assays, the strains were thawed, cultured in Potato Dextrose Broth (PDB) at 25^{o}C for 48 hours, and then inoculated onto Potato Dextrose Agar (PDA) plates to induce spore formation. The fungal strains were routinely maintained on PDA at room temperature, with subcultures performed every 20 days. To conduct the antifungal tests, spore suspensions of the pathogens were evenly spread on the surface of PDA plates using sterile cotton swabs, followed by the application of 10 µL of the extract at varying concentrations (25, 50, and 100 mg.mL^{-1}). A 10% solution of dimethyl sulfoxide

(DMSO) served as the control. The plates were then incubated at 25ºC. After 72, 96, and 144 hours of incubation, the diameter of the inhibition zones was measured to assess antifungal activity.

Analysis the component of the extract: The GC-MS analysis had been conducted using an Agilent 7890B GC system interfaced with a mass spectrometer (GC-MS) under the following conditions: A fused silica capillary column (Elite-1, 30 mm×0.25 mm ID ×1 µMdf), composed entirely of Dimethyl polysiloxane, was utilized. The instrument operated in electron impact mode at 70 eV, with Helium (99.999%) serving as the carrier gas at a constant flow rate of 1 mL.min^{-1}. Injection volume was set at 2 µL with a split ratio of 10:1, and the injector temperature was maintained at 250ºC while the ion-source temperature was set at 280ºC. The oven temperature was programmed to begin at 110°C (isothermal for 2 min), followed by a ramp of 5ºC/min up to 290ºC, and held isothermally for 10 min at 280ºC. Mass spectra were recorded at 70 eV with a scan interval of 4 min, covering fragments ranging from 40 to 600 m/z. The total runtime for the GC analysis was 59 min.

Statistical analysis

Each experiment was conducted in three replicates. Analysis of variance (ANOVA) was performed using SPSS software (ver. 20.0, IBM Corp., Armonk, New York, USA) to assess the data. The Tukey Honestly Significant Difference (HSD) test was employed to determine variations in mean values, with significance set at 5% ($p<0.05\%$).

***In silico* docking study:** For docking of ligand to enzyme, we used 2VF5: PDB collected from Protein data bank to explain why compound or pose interacted with 2VF5 enzyme that accounted for general mechanism to inhibit 2VF5 enzyme (Eze *et al.*, 2019). For anti-fungi, 4AUD protein has been used to calculate docking of ligand to protein. The activities of enzyme or protein are determined by Discovery studio visualizer 2021 software (Khan *et al.*, 2020). The numbers of model set up 1000 runs.

Results and Discussion

The main chemical compositions in rose myrtle fruit: The significant compositions of myrtle fruit are described in (Table 1). The water content in rose myrtle fruit is accounted for 78.6%, lower than grapes and apples at around 80-89% (Popkin & Rosenberg, 2010). The myrtle fruit exhibited a relatively low total sugar content (5.14 g per 100g fresh weight (FW)) compared to that of various other tropical fruits.

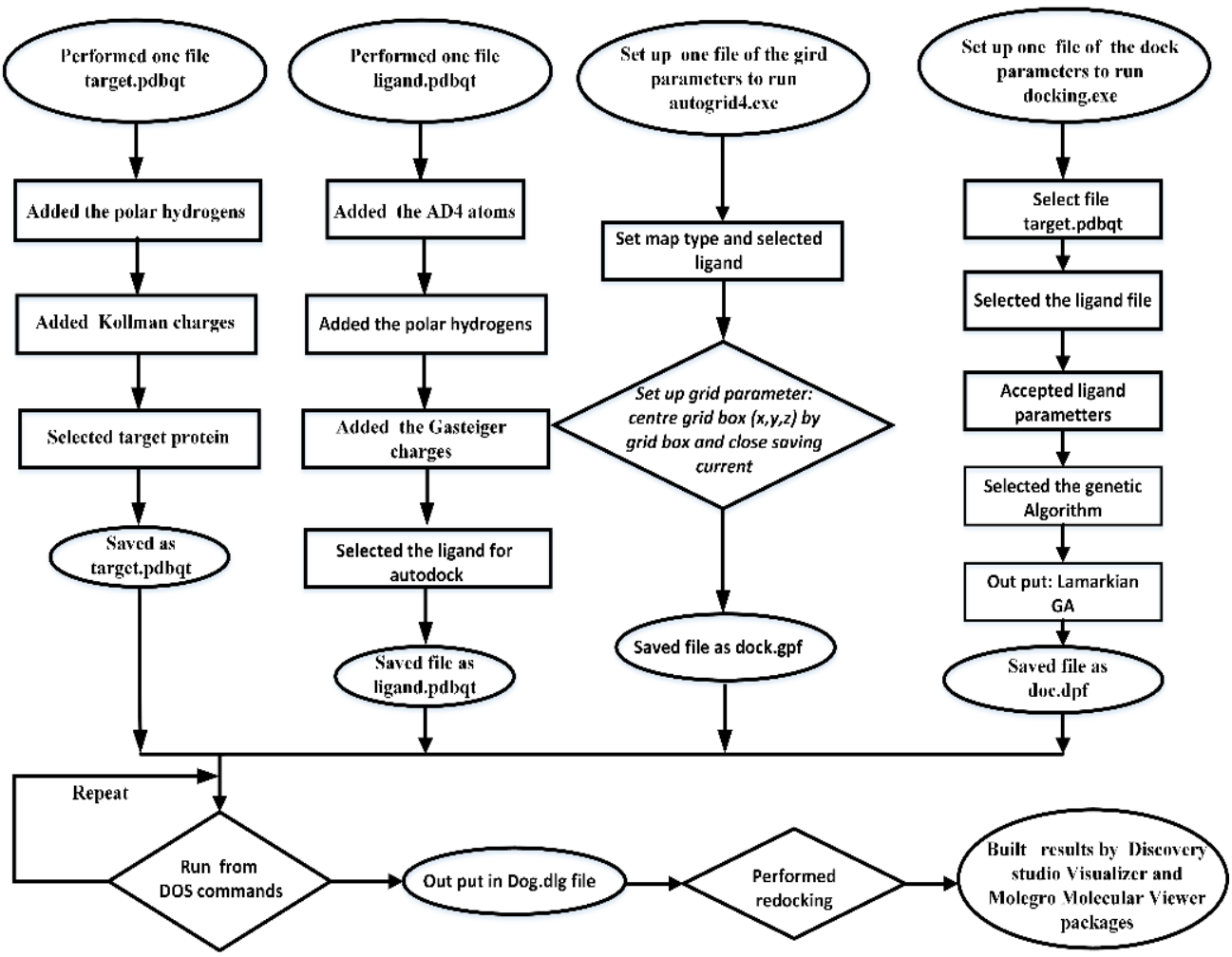

Scheme 1. The docking procedure of ligands such as compound 09, compound 12, redocking of small ligand in 2VF5 enzyme to 2VF5 enzyme, and compound 09, compound 12, redocking of small ligand in 4AUD enzyme to 4AUV enzyme.

Vitamin C content in rose myrtle accounted for 20.53 mg per 100 g of fresh weight. It is evident that vitamin C content in rose myrtle is 4 times higher than in banana (6.61 mg/100 g) and lower than pineapple (26.6 mg/100 g) (Hernández *et al.*, 2006) and strawberry (28 mg/100 g) (Moor *et al.*, 2005). The analysis of rose myrtle fruits revealed a total polyphenol content of 58,270 mg gallic acid equivalents (GAE) per 100 g and a total flavonoid content of 11,440 mg quercetin equivalents (QE) per 100 g. In comparison, similar values were observed in peaches, with total phenolic and total flavonoid contents recorded at 50.9 mg GAE/100 g and 15.0 mg QE/100 g, respectively. However, these values are notably lower than those found in blueberries, where the total phenolic and total flavonoid contents were reported as 670.9 mg GAE/100 g and 190.3 mg QE/100 g, respectively (Ribarova *et al*., 2005).

Table 1. Chemical composition of rose myrtle fruit (calculated per 100 g of fresh weight).

Chemical composition	Unit	Value
Moisture	%	78.6 ± 0.60
Total sugar (TS)	g	5.14 ± 0.09
Total acidity (TA)	g	0.203 ± 0.02
Vitamin C	mg	20.53 ± 5.08
TPC	mg GAE/g	58.270 ± 0.378
TFC	mg QE/g	11.440 ± 0.095

Effect of extraction conditions on Microware-assisted extraction of polyphenolic compounds

Effects of extraction ethanol concentration: When employing a 60% ethanol solvent for rose myrtle fruit extraction, the obtained TPC at 44.519 mg GAE/g and TFC at 7.546 mg CT/g surpassed those achieved at other ethanol concentrations. Gradual reduction in ethanol solvent concentration from 90% to 60% results in an increasing trend in both TPC and TFC content of the myrtle fruit extract; however, at 50% ethanol concentration, there is a notable decline in both TPC and TFC. This discovery resonates with the findings by Ibukunoluwa Fola Olawuyi and colleagues (Olawuyi *et al*., 2020) in their investigation concerning the extraction of polyphenolic compounds from okra (*Abelmoschus esculentus* L.) leaves, as seen in (Fig. 1).

Effects of solid: solvent ratios: Specifically, at a material to solvent ratio of 1:10, the TPC and TFC contents were 32.687 mg GAE/g and 6.193 mg CT/g, respectively. At the ratio of 1:30, a significant enhancement in TPC and TFC content was noted, reaching 51.810 mg GAE/g and 10.536 mg CT/g, respectively, corresponding to an increase of 58.50% for TPC and 47.24% for TFC. However, when the material to solvent ratio shifted from 1:30 to 1:40, the increase was only 3.86% for TPC and 2.13% for TFC, with no statistical difference was observed. This phenomenon can be ascribed to the enlarged contact area, leading to enhanced solubility and a subsequent rise in the dissolution of polyphenolics into the solvent during the process of Microwave-Assisted Extraction (MAE). The efficiency of mass transfer is acknowledged to rely on the gradient between the solid and the solvent (Belwal *et al.*, 2016); Xu *et al.*, 2017) as indicated in (Fig. 2).

Effects of extraction microwave power: The graph indicates that, under microwave treatment at a power level of 480 W, the rose myrtle fruit extract attains the highest TPC and TFC at a significance level of 5%. Specifically, the TPC is recorded at 52.379 mg GAE/g, and the TFC reaches 10.513 mg CT/g. Elevating the power from 320 W to 480 W led to an increase in the TPC and TFC in the extract, with the TPC and TFC content highest values were achieved at 480 W during microwave treatment. The observation is consistent with the results documented in an earlier investigation conducted by Xia *et al*., (2011) concerning the MAE of Oxymatrine from *Sophora flavescens*, as exposed in (Fig. 3).

Effects of extraction microwave time: Upon extending the microwave treatment duration from 3 minutes to 4 minutes, there was a notable and significant increase in the TPC and TFC within the extract (rising from 44,968 mg CT/g and 7,038 mg CT/g to 53,494 mg CT/g and 10,498 mg CT/g, respectively). However, further increases in the microwave time to 5 minutes or 6 minutes did not result in a significant augmentation of TPC or TFC content in the extract. Based on the acquired results, the extraction procedure was executed as follows: Ground powder of ripe myrtle fruit was subjected to extraction using 60% ethanol, with the specified ratios: solvent at 1:30 ($g.mL^{-1}$), microwave treatment at 480 W, and a duration of 4 minutes, as indicated in (Fig. 4).

Antioxidant activity of the rose myrtle extract: As depicted in (Fig. 5), the percentage of free radical scavenging exhibited by rose myrtle extracts and ascorbic acid varied across different concentrations. Notably, the DPPH free radical scavenging activity displayed a gradual decline with decreasing concentration. The highest observed percentage reached 72.03% at an extract concentration of 400 $\mu g.mL^{-1}$, contrasting sharply with the mere 17.83% observed at 25 $\mu g.mL^{-1}$ concentration. Utilizing the calculated values of % DPPH free radical scavenging, a graph was constructed to elucidate the correlation between scavenging activity percentage and concentration, facilitating the derivation of linear regression equations between the two variables. The resulting regression equations demonstrated a high correlation coefficient R^2 (>989%), enabling their use in calculating the IC_{50} values of the samples. The IC_{50} values for rose myrtle and ascorbic acid were determined to be 234.01 and 2.63 $\mu g.mL^{-1}$, respectively. A comparison between percentage of the free radical scavenging as seen in (Figs. 5 and 6)) revealed notable disparities in antioxidant capacity between myrtle fruit extract and the vitamin C as positive control drug. Specifically, the myrtle fruit extract (IC_{50} = 234.01 $\mu g.mL^{-1}$) exhibited substantially weaker antioxidant activity compared to vitamin C (IC_{50} = 2.63 $\mu g.mL^{-1}$), by a factor of 88.97 times. Despite this, the myrtle fruit extract demonstrated significant DPPH free radical scavenging efficacy, suggesting considerable antioxidant potential and laying the foundation for its utilization in antioxidant-functional products.

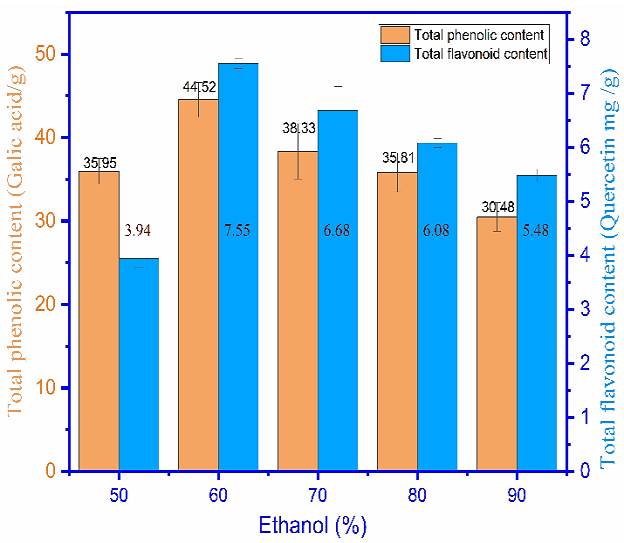

Fig. 1. Effects of extraction ethanol concentration on TPC, TFC content of ultrasonic-assisted rose myrtle fruit extract.

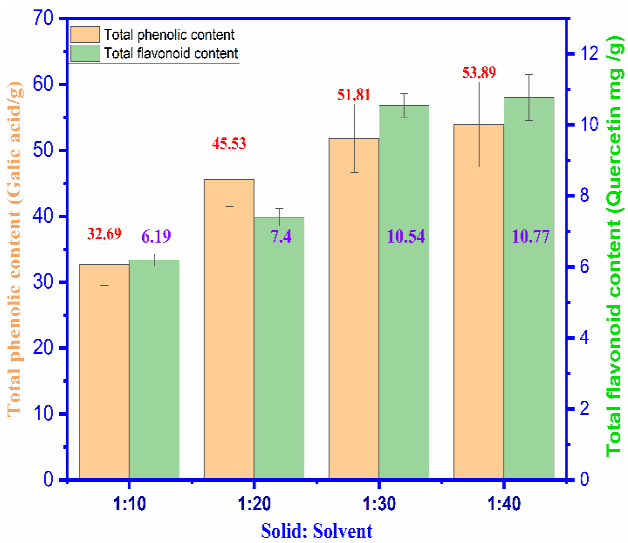

Fig. 2. Effects of solid: solvent on TPC, TFC content of ultrasonic-assisted rose myrtle fruit extract.

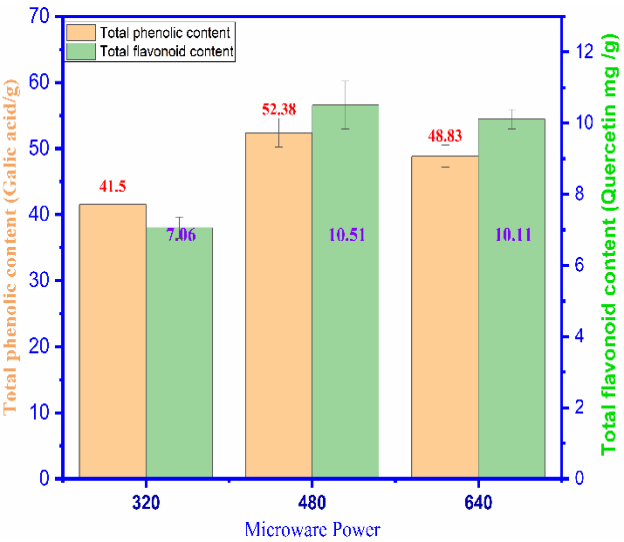

Fig. 3. Effects of microware power on TPC, TFC content of ultrasonic-assisted rose myrtle fruit extract.

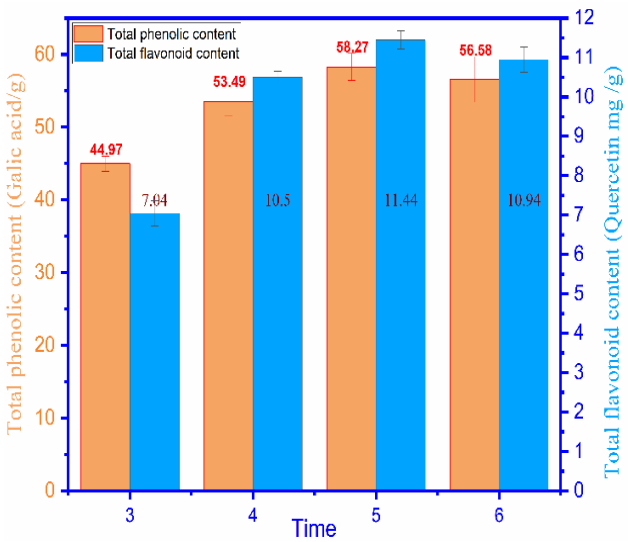

Fig. 4. Effects of extraction time on microwave on TPC, TFC content of ultrasonic-assisted rose myrtle fruit extract.

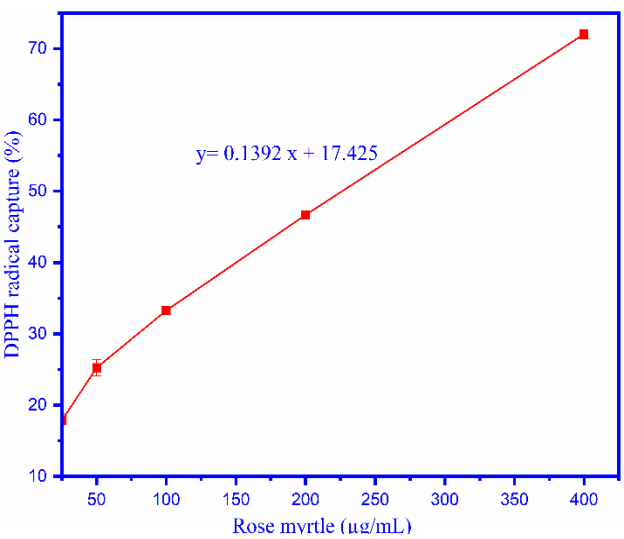

Fig. 5. Percentage of free radical scavenging of rose myrtle extracts.

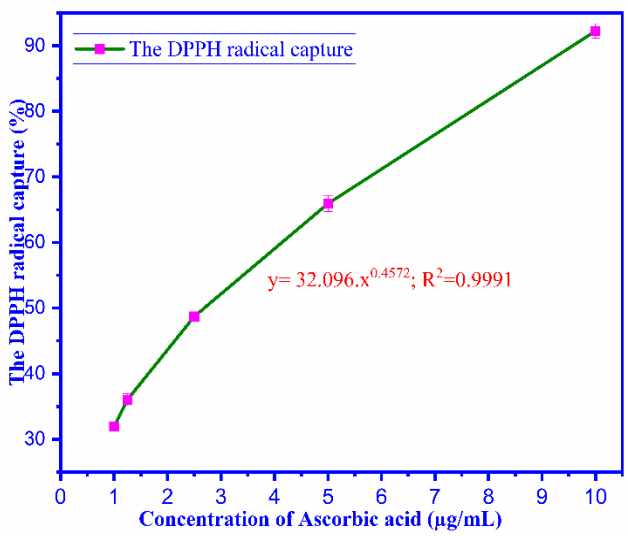

Fig. 6. Percentage of free radical scavenging of Ascorbic acid at different concentrations.

Evaluation of the antibacterial ability of the extract: After 24 hours of culture in the 37°C incubator, the agar plates were removed to determined the results of antibacterial activity of myrtle extract as indicated in (Table 2). The antibacterial ability of the myrtle extract was determined based on its ability to inhibit the growth of bacteria, as shown by the diameter (mm) of the antibacterial ring created on the petri dish.

Research results show that the ethanol extract of myrtle fruit has the ability to inhibit the growth of both evaluated bacterial strains. The degree of resistance depends on the concentration of the extract used. The best resistance effect on *E. coli*., at a concentration of 500 mg.mL^{-1}, the antibacterial ring diameter for *E.coli* was 6.73 ± 0.90 mm and the antibacterial ring diameter for *Salmonella sp.* is 4.80 ± 0.75 mm. Even at a low concentration of 125 mg.mL^{-1}, antibacterial activity was also shown on *E.coli*, while with *Salmonella sp.* there was no antibacterial ring. From the results of the ability to inhibit the growth of *E.coli* and *Salmonella* sp., it was evident that myrtle fruit was a suitable source of raw materials for the research direction of products that have the effect of preventing and treating diarrhea in humans and animals. From that result, it can be seen that the antibacterial activity of *E. coli* and *Salmonella* sp. Of ethanol extract of myrtle fruit was much lower than that of the n-butanol extract of the small-leaved plant. The findings from this investigation agree to the research conducted by Jabri *et al*., (2016) regarding the effects of myrtle berries extract, demonstrating a notable dose-dependent protection against diarrhea and intestinal fluid accumulation.

Table 2. The antibacterial activity of myrtle extract against *E. coli* and *Salmonella* sp.

Concentration (mgmL^{-1})	Inhibition zone (mm)	
	***Salmonella* sp.**	***E. coli***
500	4.80 ± 0.75	6.73 ± 0.90
250	2.63 ± 0.50	3.73^{b} ± 0.60
125	-	2.27^{c} ± 0.40
62.5	-	-
Distilled water	-	-

***In vitro* antifungal activity:** As seen in (Fig. 7), the antimicrobial activity of rose myrtle fruit extract agianst *Alternaria alternata* apple pathotype indicated at concentrations of 25 mg.mL^{-1}, 50 mg.mL^{-1}, and 100 mg.mL^{-1} excellent activites. This novel results of this projects and this can be considered that the concentration of 25 mg.mL^{-1} is MIC value of rose myrtle fruit extract. The antifungal activity of the rose myrtle fruit extract has been conducted against three fungal strains responsible for diseases in Japanese pears and apples. The myrtle fruit extract at concentrations of 50 and 100 mg.mL^{-1}, has shown the ability to inhibit the growth of *Alternaria citri* fungus after 72, 96, and 144 hours of incubation as seen in (Fig. 8A-C), respectively.

Analysis of the chemical composition of the extract: The GC-MS method with the HP5-MS column has conducted to separate 19 compounds in the ethanol extract of myrtle fruit and there are only three compounds being identified clearly. Among the identified compounds, as seen in (Table 3), it is noteworthy that 2,3-Dihydro-3,5-dihydroxy-6-methyl-4H-pyran-4-one (compound 9) belongs to the flavonoid group of substances that slow down the oxidation process caused by free radicals, thereby preventing cancer, atherosclerosis, cerebrovascular accidents, liver degeneration, radiation damage, stabilizing blood pressure, and protecting liver function. Another one is 5-Hydroxymethylfurfural (compound 12)

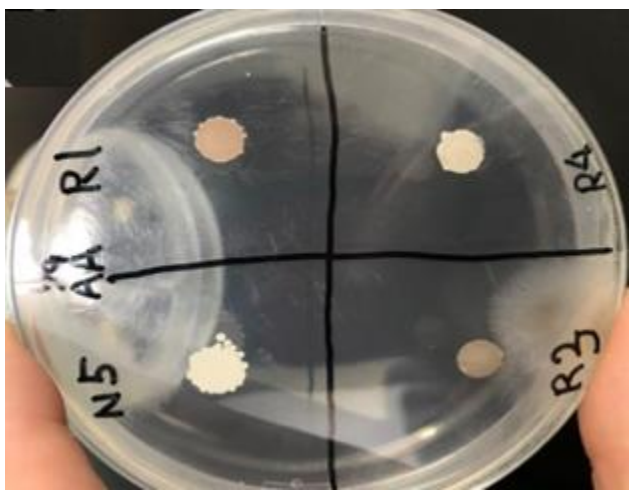

Fig. 7. The antimicrobial activity of rose myrtle fruit extract agianst *Alternaria alternata* apple pathotype at the differentical concentrations.

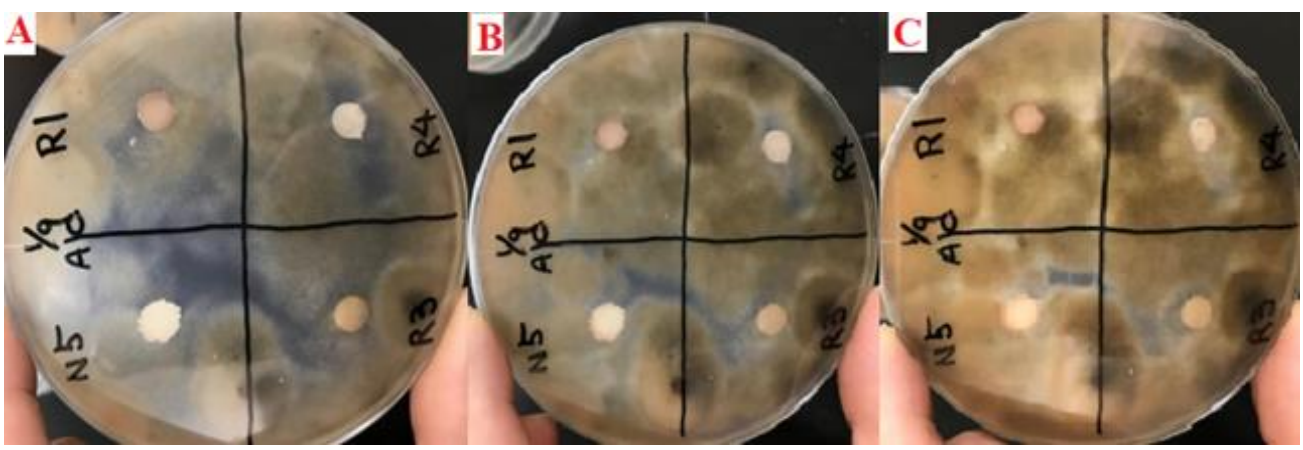

Fig. 8. Agar diffusion test of the rose myrtle fruit extract. The picture shows the halos of the antifungal activity at the different concentrations R1 (25 mg.mL^{-1}), R3 (50 mg.mL^{-1}) and R4 (100 mg.mL^{-1}) of the rose myrtle fruit extract and in comparison with the "N5" control (10% DMSO) on *Alternaria citri: 8*A. 72 h; 8B. 96 h, and 8C. 144 h.

Table 3. Chemical composition of the extract of myrtle fruit.

Compound	Retention time [a]	Peak area % [b]	Composition
1	4.186	5.337	(-)
2	4.558	1.727	(-)
3	5.004	1.904	(-)
4	5.983	1.894	(-)
5	7.296	1.856	(-)
6	9.056	1.023	(-)
7	9.142	1.716	(-)
8	10.121	1.562	(-)
9	**11.868**	**7.758**	**2,3-Dihydro-3,5-dihydroxy-6-methyl-4H-pyran-4-one**
10	13.008	0.913	(-)
11	13.380	1.708	(-)
12	**14.296**	**20.538**	**5-Hydroxymethylfurfural**
13	16.712	4.184	(-)
14	18.472	2,425	(-)
15	25.521	7.125	(-)
16	29.362	0.919	(-)
17	31.134	1.543	(-)
18	38.865	2.995	(-)

[a]: Retention time, min; [b]: The % area result is the ratio of the area of the component peak in the GC-MS chromatogram to the total peak area of the relevant substances in the selected chromatogram

***In silico* docking study such as antibacteria, antioxidant, antifungi and anticancer activities**

Anti bacterial activity

Compound 12 or pose 505: pose 505/1000 docked to 2VF5 with the valuses of Free Gibbs energy and inhibition constant of -4.18 and 0.86 mM as indicated in (Table 4) and this pose forms with 2VF5 enzyme with 4 hydrogen bonding such as X:Thr 302:N – Pose 505:O (2.83 Å), X:Ser 303:N – Pose 505:O (2.87 Å), X:Ser 303:O – Pose 505:O (2.94 Å), Pose 505:H - X:Cys 300:O (2.07 Å) as showed in (Table 4). Among us, the hydrogen bonding, Pose 505:H - X:Cys 300:O (2.07 Å) is the most stable because of shortest bonding length. The interaction profile of pose 505 and 2VF5 enzyme has been demenstrated as shown in (Fig. 9A-E). As see in (Fig. 9A), the H-bonds (donor and accepter) between pose 505 and 2VF5 are predented and showed pose 505 having 2 areas of donor and accepter of H-bonding. As indicated in Fig. 9B, compound 12 reveals higher polarity in blue areas. As exposed in (Fig. 9C), it is evident that pose 505 effectively interacts with the 2VF5 enzyme, with three key interactions: Thr 355 to the oxygen atom of the carbonyl group, Cys 300 to the hydrogen atom of the alcohol group, and Thr 302 to the oxygen atom of the alcohol group (-CH_2OH). Additionally, two hydrophobic interactions are identified from Ser 303 and Gln 348 to the pi system on the five-member ring of pose 505. The ligand interactions between pose 505 and 2VF5 are further illustrated in the 3D diagram presented in (Fig. 9D), mirroring the 2D interactions depicted in (Fig. 9C). Furthermore, as seen in (Fig. 9E), the secondary interactions are presented, including hydrogen bonding with Arg 599, steric interactions with Leu 601, Tyr 491, Ile 492, Lys 487, and His 493, as well as overlapping interactions indicated by violet circles on the pose. The size of the violet circles signifies the strength of the overlap interactions, with more significant steric interactions around the pose indicating strong interactions between pose 505 and the residual amino acids on the enzyme. Pose 505 docks effectively to the enzyme, elucidating why compound 12 demonstrates promising antimicrobial activity *in vitro*. Compound 9 or pose 429 out of 1000, interacts with 2VF5 as outlined in (Table 4) and (Fig. 10A-F). However, (Fig. 10E) indicates that pose 429 does not dock effectively with enzyme 2VF5, exhibiting only one hydrogen bonding from Asn 522 to the oxygen atom of the carbonyl group on pose 429. As exposed in (Fig. 11A-D), and (Table 4), the small ligands in 2VF5 or pose 384 interact well with 2VF5 and pose 384 serves as one small ligand that effectively anchors to the enzyme.

Anti fungi i*n silico*: The docking analysis of 2,3-Dihydro-3,5-dihydroxy-6-methyl-4H-pyran-4-one, also known as compound 12 or pose 698 out of 1000, has been anchored to the 4AUD protein. The free Gibbs energy and inhibition constant are recorded as -4.30 kcal.mol^{-1} and 708 mM, respectively, as presented in (Table 4). Pose 698 also formed two hydrogen bonds: A:Lys 58:N – Pose 698:O (3.00 Å) and Pose 698:H - A:Glu 55:O (1.78 Å). The interaction profile between pose 698 and the 4AUD protein has been demonstrated in (Fig. 12A-D). Pose 698 exhibits characteristics of both donor and acceptor of hydrogen bonds, as seen in (Fig. 12A) and appears to be more hydrophilic than hydrophobic, as indicated in (Fig. 12B). The interaction of pose 698 with 4AUD protein is evident in (Fig. 12), where significant ligand interactions are depicted in a 3D diagram, and the 2D ligand interactions as seen in (Fig. 12C). Furthermore, as inicated in (Fig. 12E) illustrates the secondary interactions between pose 698 and

4AUD, including hydrogen bonding with Glu 55 and Lys 58, steric interactions with Tyr 280, Phe 72, Glu 55, and Asp 56, and overlap interactions identified by violet circles on the pose. The best docking pose 272 among 1000 docking conformations of 5-hydroxymethylfurfural or compound 9, interacts with the 4AUD protein with a free Gibbs energy of -4.62 kcal.mol^{-1} and an inhibition constant of 413 mM, as indicated in (Table 4). However, the interaction profiles in (Fig. 13A-D) demonstrate that pose 272 does not interact effectively with 4AUD: PDB, displaying only one hydrogen bond from Glu 55 to the oxygen atom of the ketone group. Another ligand, pose 64 among 1000 poses has been demonstrated in 4AUD: PDB and docked to the 4AUD protein with a free Gibbs energy of -3.74 kcal.mol^{-1} and an inhibition constant of 1.81 mM, as seen in Table 4. The significant ligand interactions of pose 64 and 4AUD has been indicated in (Fig. 14A) on 3D diagram. Pose 64 has been demonstrated effective interaction with 4AUD in the ligand interaction model, displaying both donor and acceptor attributes of hydrogen bonds in (Fig. 14B). Additionally, pose 64 appears to be more hydrophilic than hydrophobic, as depicted in (Fig. 14C) that blue color part around this pose is more that of another part.

Table 4. The significant docking results of pose 429 (compound 09), pose 505 (compound 12) to 2VF5 enzyme; PDB to explain the inhibition enzyme mechanism *in silico* via synthesis inhibition of cell walls via 2VF5 enzyme inhibition.

Compound [a]	Pose[b]	Enzyme: PDB[c]	ΔG[d]	K [e]	The number of hydrogens [f]	The character and bond length[g]
Anti-bacteria: 2VF5 enzyme: PDB						
09	429/1000	2VF5	-3.91	1.36	1	Asn 522: N- Pose 429 (3.16 Å)
12	505/1000	2VF5	-4.18	0.86	4	X: Thr 302: N – Pose 505:O (2.83 Å) X: Ser 303: N – Pose 505:O (2.87 Å) X: Ser 303:O – Pose 505:O (2.94 Å) Pose 505:H - X: Cys 300:O (2.07 Å)
Small ligand in 2VF5	384	2VF5	-4.53	0.48	-	-
Anti-fungi: 4AUD protein: PDB						
09	272	4AUD	-4.62	413	1	A: Glu 55: N – Pose 272:O (2.78 Å)
12	698/1000	4AUD	-4.30	708	2	A: Lys 58: N – Pose 698:O (3.00 Å) Pose 64: H – A: Glu 55:O (1.78 Å)
Small ligand in 4AUD	64/1000	4AUD	-3.74	1.81	-	-

[a]: Compound extracted and identified from GC-MS as seen in Table 3; [b]: The best docking pose among 1000 conformation of compound; [c]: It is collected from protein data bank; [d], [e]: The results from docking caculations via Autodock tool, [f], [g]: It has been build from DSC software

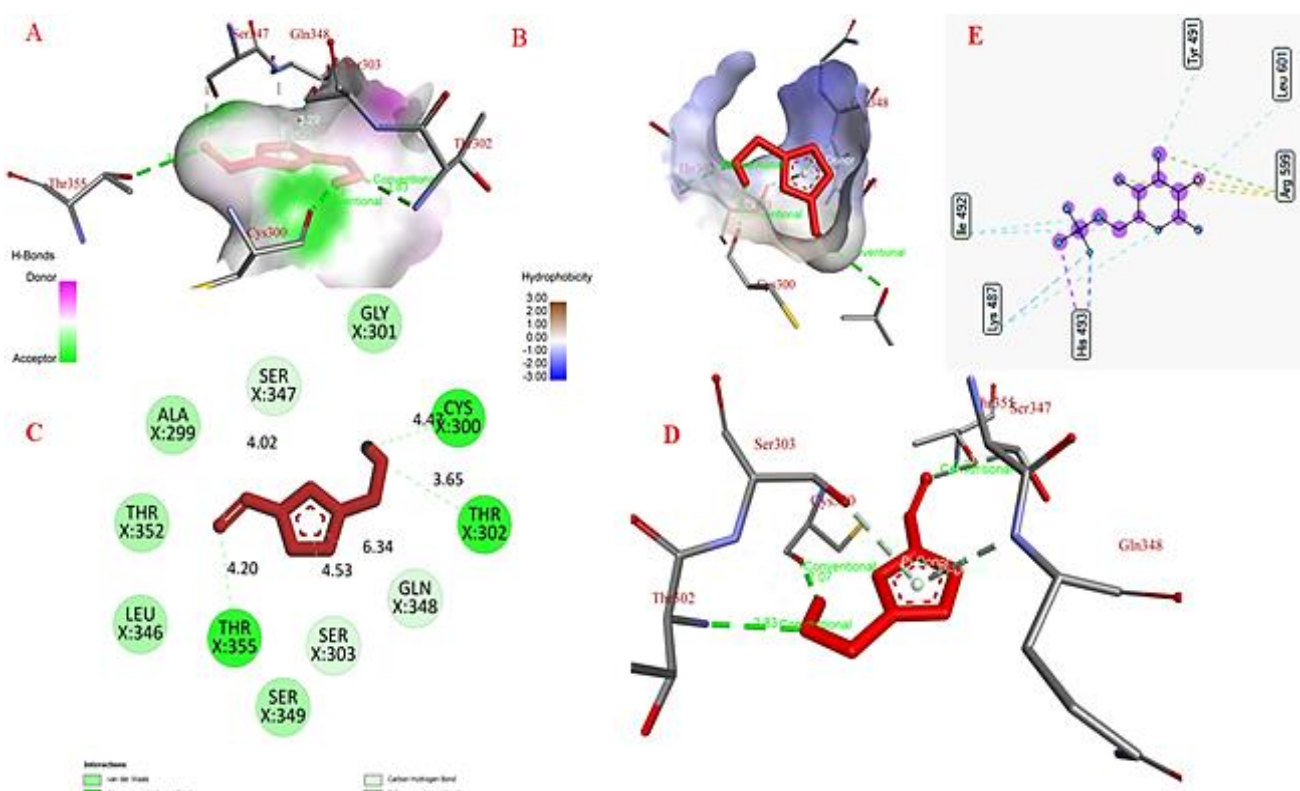

Fig. 9. The docking profile of 5-Hydroxymethylfurfural or pose 505/1000, the best conformation of compound 12 to 2VF5 enzyme: PDB to explain the antimicrobial activity mechanism *in silico* study.

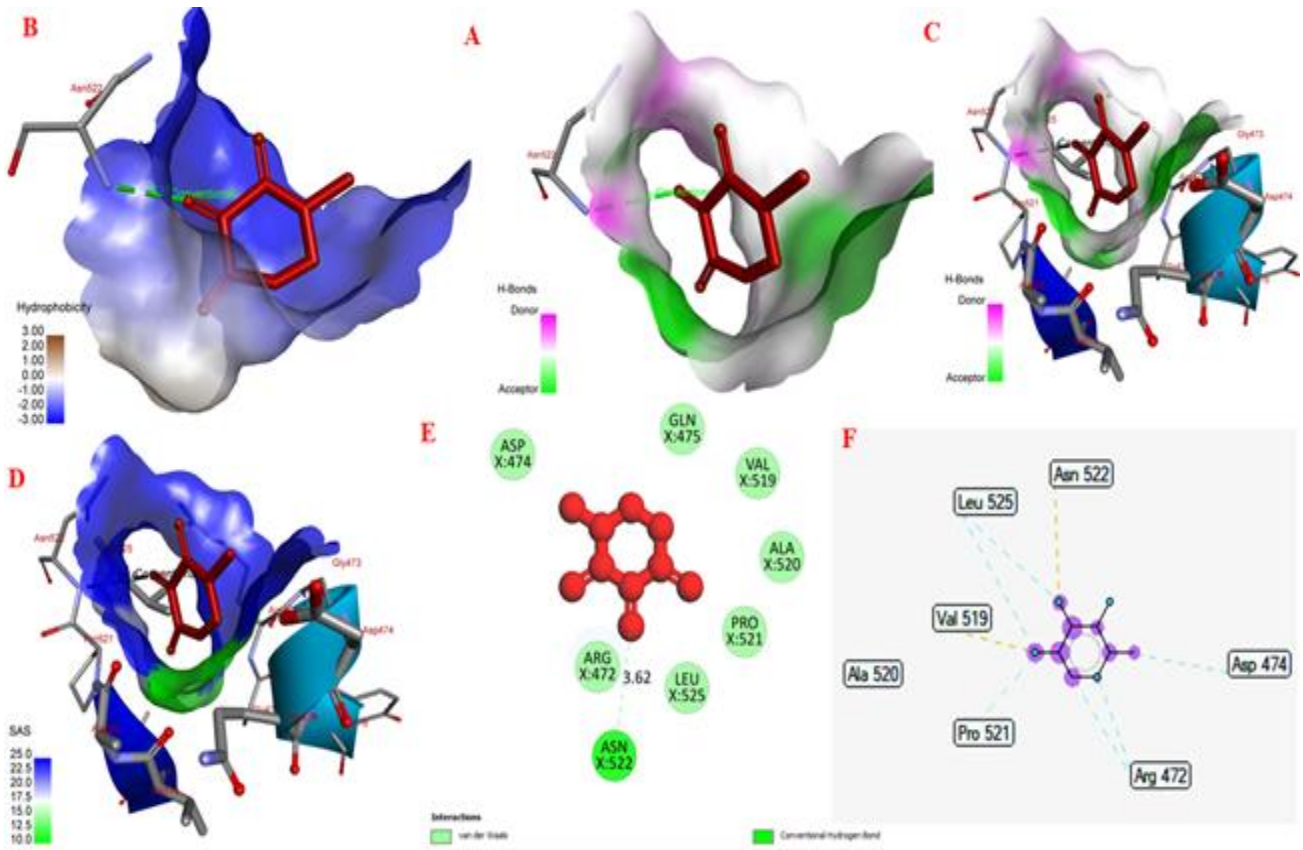

Fig. 10. The docking profile of 2,3-Dihydro-3,5-dihydroxy-6-methyl-4H-pyran-4-one compound 9 or one docking pose 429/1000, the best conformation of compound 12 to 2VF5 enzyme: PDB to explain the antimicrobial activity mechanism *In silico* study.

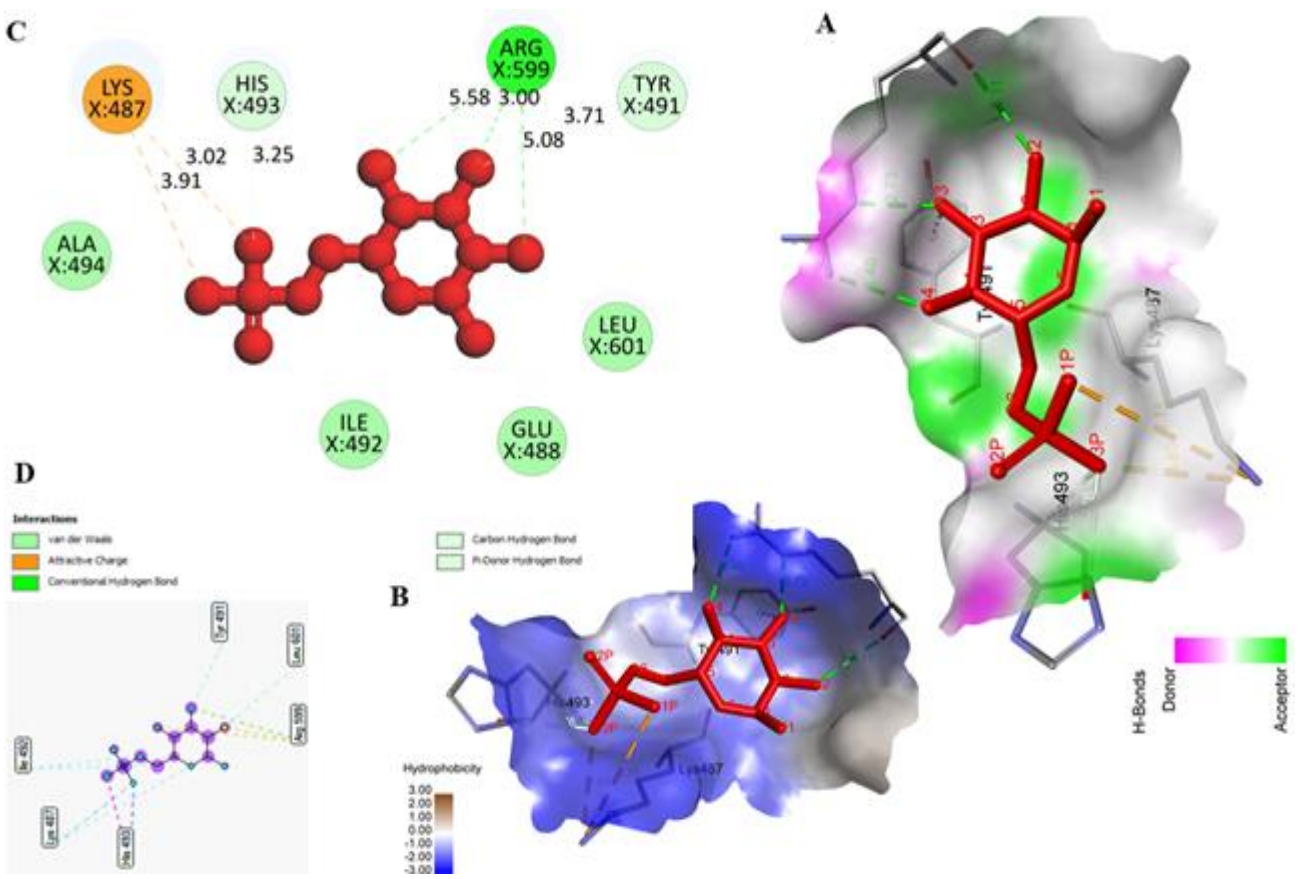

Fig. 11. The docking profile of small ligand in 2VF5 or one docking pose 384/1000, the best conformation of small ligand to 2VF5 enzyme: PDB to explain the antimicrobial activity mechanism *In silico* study.

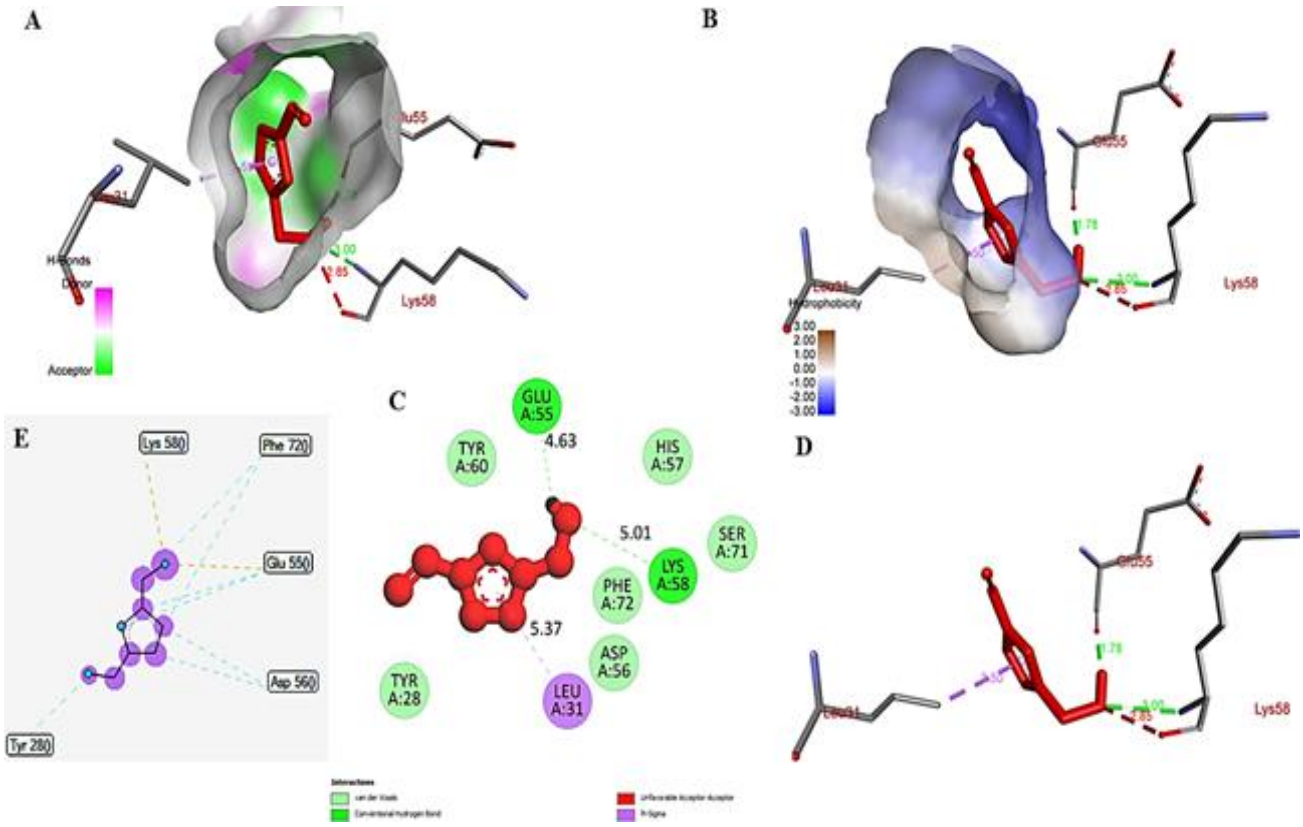

Fig. 12. The docking profile of 2,3-Dihydro-3,5-dihydroxy-6-methyl-4H-pyran-4-one or compound 12, or one docking pose 698/1000, the best conformation of compound 12 to 4AUD: crystal structure of alternaria alternata: PDB to explain the antimicrobial activity mechanism *In silico* study.

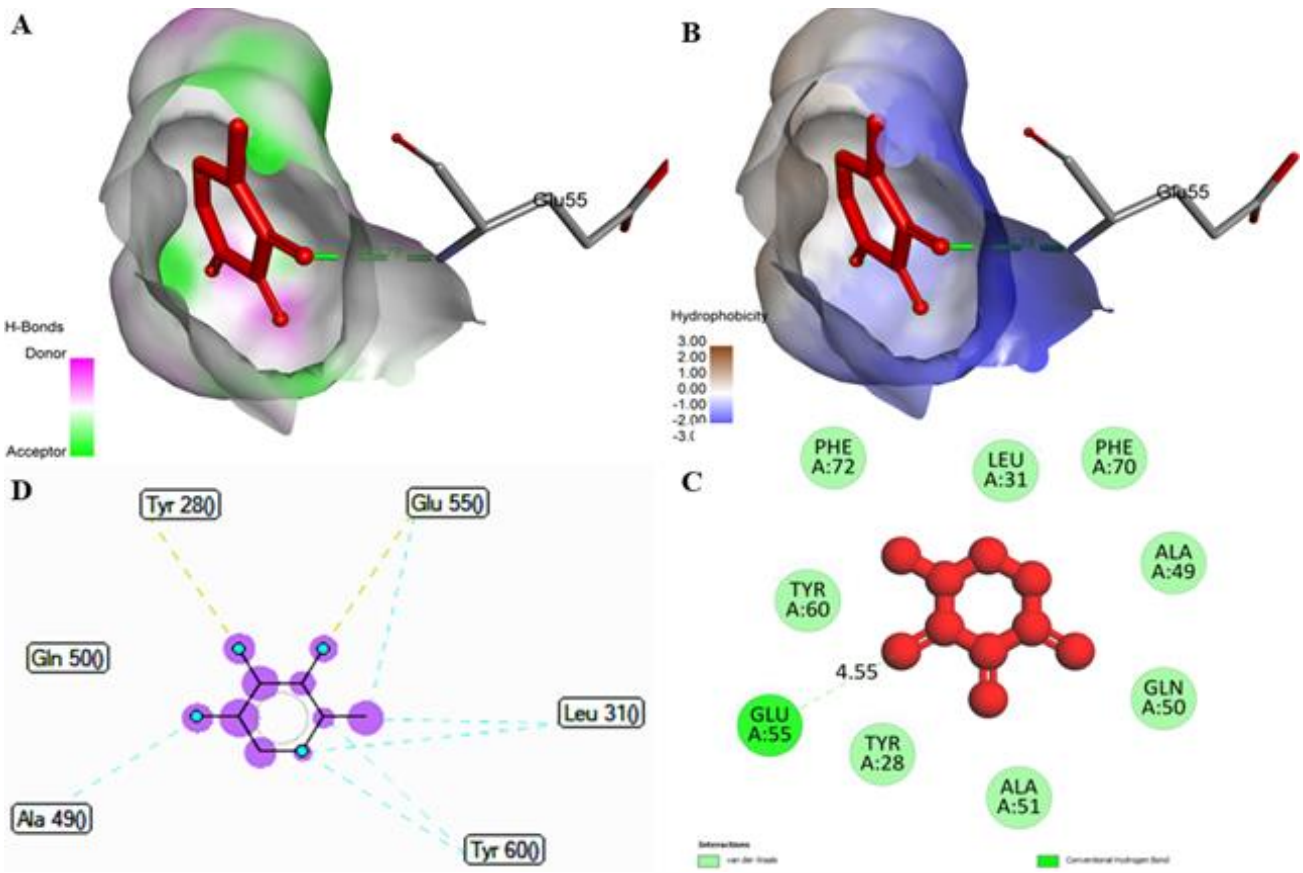

Fig. 13. The docking profile of 5-hydroxymethylfurfural/compound 9, or one docking pose 272/1000, the best conformation among them to 4AUD: crystal structure of alternaria alternata: PDB to explain the antimicrobial activity mechanism *In silico* study.

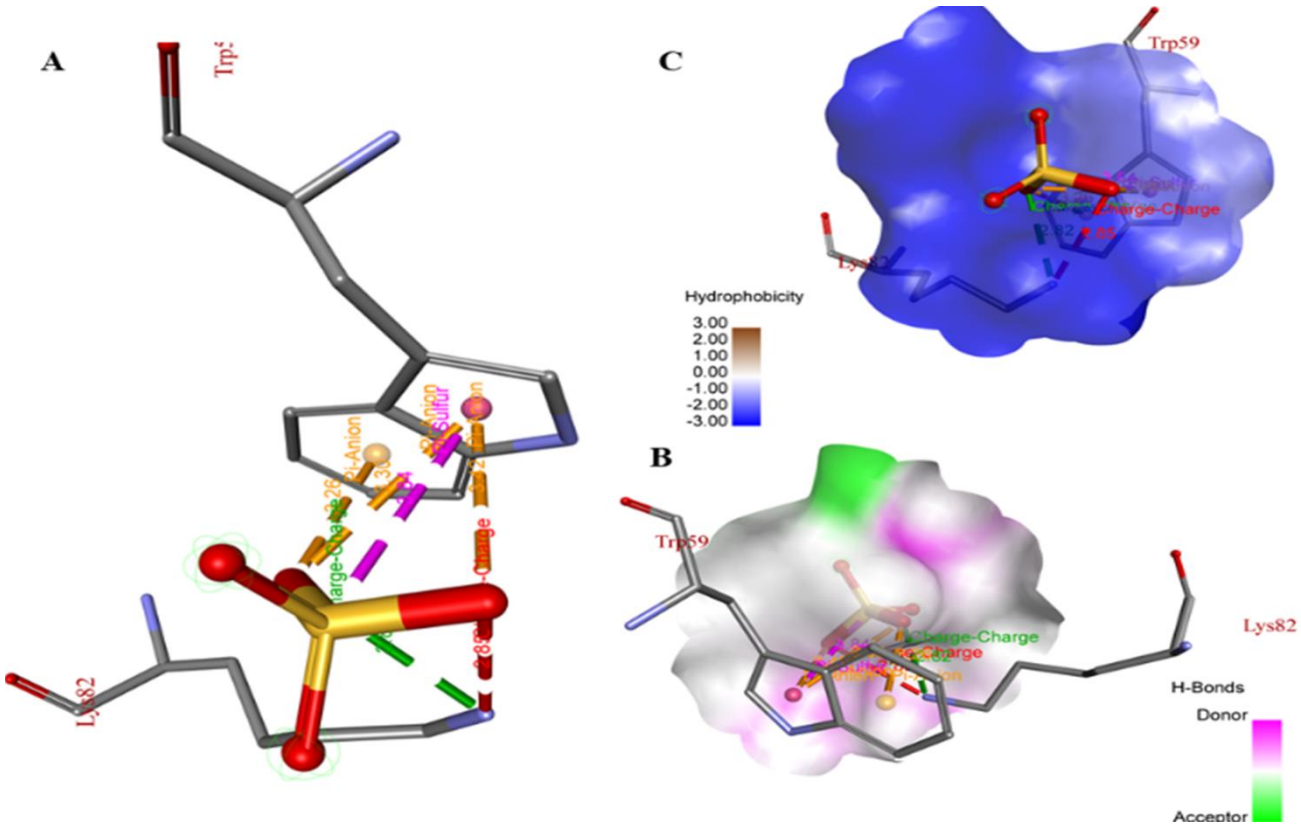

Fig. 14. The docking profile of small ligand in 4AUD, or one docking pose 64/1000, the best conformation among them to 4AUD: crystal structure of alternaria alternata: PDB to explain the antimicrobial activity mechanism *In silico* study.

Conclusion

The antioxidant potential of myrtle fruit extract was assessed using the DPPH radical inhibition assay. The IC_{50} value of the myrtle extract was determined to be 233.98 µg.mL^{-1}, indicating weaker antioxidant activity compared to vitamin C. Additionally, the antibacterial efficacy of myrtle extract was evaluated against *Escherichia coli* and *Salmonella*, revealing promising activities. Using GC-MS with an HP5-MS column, various biologically active compounds in the myrtle extract were identified. Notably, 2,3-dihydro-3,5-dihydroxy-6-methyl-4H-pyran-4-one was detected in the myrtle extract. The novel antifungal activity of rose myrtle fruit extract against *Alternaria alternata* apple pathotype was observed at MIC concentrations of 25 mg.mL^{-1}, demonstrating excellent efficacy. *In silico* docking studies revealed that pose 698 out of 1000, corresponding to compound 12, exhibited strong binding affinity to the 4AUD:PDB protein, while compound 12 or pose 505 effectively inhibited the 2VF5:PDB enzyme. Microwave-assisted extraction was employed to extract rose myrtle fruit highlighting the dependence of the fruit extract's components on solvent polarity, solid-to-solvent ratio, microwave power, and treatment duration.

References

Abraham, M.J., T. Murtola, R. Schulz, S. Páll, J.C. Smith, B.Hess and E. Lindahl. 2015. Gromacs: High performance molecular simulations through multi-level parallelism from laptops to supercomputers. SoftwareX., 1: 19-25. doi: 10.1016/j.softx.2015.06.001.

Agrawal, P., H. Singh, H.K. Srivastava, S. Singh, G. Kishore and G.P.S. Raghava. 2019. Benchmarking of different molecular docking methods for protein-peptide docking. *BMC Bioinform.*, 19: 106-124. doi: 10.1186/s12859-018-2449-y.

Ash, J. and D. Fourches. 2017. Characterizing the chemical space of ERK2 Kinase inhibitors using descriptors computed from molecular dynamics trajectories. *J. Chem. Inf. Model.*, 57: 1286-1299.

Bell, E.W. and Y. Zhang. 2019. DockRMSD: An open-source tool for atom mapping and RMSD calculation of symmetric molecules through graph isomorphism. *J. Chem.* 11: 1-9. doi: 10.1186/s13321-019-0362-7.

Belwal, T., P. Dhyani, I.D. Bhatt, R. Rawal and V. Pande. 2016. Optimization extraction conditions for improving phenolic content and antioxidant activity in Berberis asiatica fruits using response surface methodology (RSM). *Food Chem.*, 207: 115-124.

Chang., C., M. Yang, H. Wen and J. Chem. 2002. Estimation of, flavonoid total content in propolis by two complementary colorimetric methods. *J. Food Drug Anal.*, 10: 178-182.

Cos, P., A.J. Vlietinck, D. Vanden Berghe and L. Maes. 2006. Anti-infective potential of natural products: How to develop a stronger *In vitro* 'proof-of-concept. *J. Ethnopharmacol.*, 106: 290-302.

Dachriyanus, Salni, M.V. Sargent, B.W. Skelton, I. Soediro, M. Sutisna, Allan White and E. Yulinah. 2002. Rhodomyrtone, an antibiotic from *Rhodomyrtus tomentosa*. *Aust J. Chem.*, 55: 229-232.

Duy, N., T. Ha, T. Phuong and T.N.M. An. 2023. Novel Benzimidazol-2-Thione Derivatives: Synthesis, *In vitro* anticancer, antimicrobial activities, and *In Silico* molecular docking study. *Chem. Select*, 202300246: 2-13.

Ece, A. 2023. Computer-aided drug design. *BMC Chem.*, 17: 1-3. doi: 10.1186/s13065-023-00939-w.

Eze, F.U., U.C. Okoro, D.I. Ugwu and S.N. Okafor. 2019. Biological activity evaluation of some new benzenesulphonamide derivatives. *Front Chem*., 7: 1-12.

Hamid, H.A., R. Mutazah and M. Yusoff. 2016. *Rhodomyrtus tomentosa*: A phytochemical and pharmacological review. *Asian J. Pharm. Clin. Res.*, 10: 10-16.

Hernández, Y., M.G. Lobo and M. González. 2006. Determination of vitamin C in tropical fruits: A comparative evaluation of methods. *Food Chem*., 96: 654-664.

Hudzicki, J. 2009. Kirby-Bauer disk diffusion susceptibility test protocol. *Amer. Soc Microbiol.* https://asm.org/getattachment/2594ce26-bd44-47f6-8287-0657aa9185ad/Kirby-Bauer-Disk-Diffusion-Susceptibility-Test-Protocol-pdf.pdf. Accessed 08 Dec 2023.

Huey, R., G.M. Morris and S. Forli. 2012. Using autodock 4 and autodock vina with autodocktools: a tutorial. http://autodock.scripps.edu/faqs-help/tutorial/using-autodock-4-with-autodocktools/2012_ADTtut.pdf. Accessed 12 Dec 2023.

Jabri, M.A., K. Rtibi, A. Said, C. Aouadhi, K. Hosni, M. Sakly and H. Sebai. 2016. Antidiarrhoeal, antimicrobial and antioxidant effects of myrtle berries (*Myrtus communis* L.) seeds extract. *J. Pharm. Pharmacol.*, 68: 264-274. doi: 10.1111/JPHP.12505.

Khan, S.U., N. Ahemad, L.H. Chuah, R. Naidu and T.T. Htar. 2020. Illustrated step by step protocol to perform molecular docking: Human estrogen receptor complex with 4-hydroxytamoxifen as a case study. *Prog. Drug Discov. Biomed. Sci.*, 3(1): doi: 10.36877/pddbs.a0000054.

Kita, Y., Y. Miura and K. Yagasaki. 2012. Antiproliferative and anti-invasive effect of Piceatannol, a polyphenol present in grapes and wine, against hepatoma AH109A cells. *J. Biomed. Biotechnol*., doi: 10.1155/2012/672416.

Kwon, J.Y., S.G. Seo, Y.S. Heo, S. Yue, J.X. Cheng, K.W. Lee and K.H. Kim. 2012. Piceatannol, natural polyphenolic stilbene, inhibits adipogenesis via modulation of mitotic clonal expansion and insulin receptor-dependent insulin signaling in early phase of differentiation. *J. Biol. Chem*., 287:11566. doi: 10.1074/JBC.M111.259721.

Lai, T.N.H., M.F. Herent, J. Quetin-Leclercq, T.B.T. Nguyen, H. Rogez, Y. Larondelle and C.M. André. 2013. Piceatannol, a potent bioactive stilbene, as major phenolic component in *Rhodomyrtus tomentosa*. *Food Chem.*, 138: 1421-1430.

Li, H.B., K.W. Cheng, C.C. Wong, K.W. Fan, F. Chen and Y. Jiang. 2007. Evaluation of antioxidant capacity and total phenolic content of different fractions of selected microalgae. *Food Chem.*, 102: 771-776.

Lim, T.K. 2012. *Fruits*. Vol: 3. Edible Medicinal And Non Medicinal Plants.doi: 10.1007/978-94-007-2534-8

Limsuwan, S. and S.P. Voravuthikunchai. 2008. *Boesenbergia pandurata* (Roxb.) Schltr., *Eleutherine americana* Merr. and *Rhodomyrtus tomentosa* (Aiton) Hassk. as antibiofilm producing and antiquorum sensing in *Streptococcus pyogenes*. *FEMS Immunol. Med. Microbiol.*, 53: 429-436.

Mai, T.C., N.T. Tran, D.T. Mai, T.C. Mai, N.T. Tran, D.T. Mai, T.T.N. Mai, N.H.T. Duyen, T.N.M. An, M. Alam, C.H. Dangab and T.D. Nguyen. 2022. Supercritical CO2 assisted extraction of essential oil and naringin from *Citrus grandis* peel: *In vitro* antimicrobial activity and docking study. *RSC Adv*., 12: 25962-25976.

Moor, U., K. Karp, P. Põldma and A. Pae. 2005. Cultural systems affect content of anthocyanins and vitamin C in strawberry fruits. *Europ. J. Hort. Sci.*, 70: 1611-4426.

Morris, G.M., D.S. Goodsell, M.E. Pique, W.L. Lindstrom, R. Huey, S. Forli, W.E. Hart, S. Halliday, R. Belew and A.J. Olson. 2009. AutoDock4 and AutoDockTools4: Automated docking with selective receptor flexibility. *The J. Comp. Chem.*, https://doi.org/10.1002/jcc.21256.

Nguyen, H.H., N.M.A. Tran, T.H.T. Nguyen, H.C. Vo, C.H. Nguyen, T.H.A. Nguyen, N.H. Nguyen and T.H. Duong. 2022. Rotenoids and coumaronochromonoids from *Boerhavia erecta* and their biological activities: *In vitro* and *In silico* studies. *J. Saudi Chem. Soc.*, 26: 101489.

Nguyen, H.T., T.T. Nguyen, T.H. Dương, N.T.T. Hai, L.T. Hieu, T.T. Hoa, H.T.P. Loan, N.T. Triet, T.T.V. Anh, P.T. Quy, P.V. Tat, N.V. Hue, D.T. Quang, N.T. Trung, V.T. Tung, L.K. Huynh and N.T.A. Nhung. 2022. α-Glucosidase inhibitory and antimicrobial benzoylphloroglucinols from *Garcinia schomburgakiana* fruits: *In vitro* and *In silico* Studies. *Molecules*, 27(8): doi: 10.3390/molecules27082574.

Olawuyi, I.F., J.J. Park and W.Y. Lee. 2020. Effect of extraction conditions on ultrasonic-Assisted extraction of polyphenolic compounds from okra (*Abelmoschus esculentus* L.) leaves. *Korean J. Food Preserv.*, 27: 476-486. doi: 10.11002/KJFP.2020.27.4.476.

Pham, T.N.T, T.T. Nguyen, T.L.T. Nguyen, M.N.T. An, T.N. Nguyen, D.T. Tong and D.T. Le. 2022. Antioxidant and anti-inflammatory activities of phytochemicals from *Ruellia tuberosa*. *J. Chem.*, doi: 10.1155/2022/4644641.

Plank, D.W., J. Szpylka, H. Sapirstein, D. Woollard, C.M. Zapf, V.L., C.Y.O. Chen, R.H. Liu, R. Tsao, A.Düsterloh and S. Baugh. 2012. Determination of antioxidant activity in foods and beverages by reaction with 2,2′-Diphenyl-1-Picrylhydrazyl (DPPH): Collaborative study first action 2012.04. *J. AOAC Int.*, 95: 1562-1569.

Popkin, B.M. and D.K. Rosenberg. 2010. Water, hydration and health. *Nutr Rev.*, 68:439.

Ribarova, F., D. Marinova, F. Ribarova and M. Atanassova. 2005. Total phenolics and flavonoids in Bulgarian fruits and vegetables. *J. Univ. Chem. Technol. and Metallurgy*, 40: 255-260.

Ravindranath, P.A., S. Forli, D.S. Goodsell, A.J. Olson and M.F. Sanner. 2015. AutoDockFR: Advances in protein-ligand docking with explicitly specified binding site flexibility. *PLoS Comput. Biol.*, 11: 1-28.

Shaw Research DE 2011. Desmond Version 3.0 Tutorial. https://www.deshawresearch.com/downloads/download_desmond.cgi/Desmond_Tutorial-0.6.pdf Accessed 10 Dec 2023.

Saising, J., A. Hiranrat, W. Mahabusarakam, M. Ongsakul and S. Voravuthikunchai. 2008. Rhodomyrtone from *Rhodomyrtus tomentosa* (Aiton) Hassk. as a natural antibiotic for staphylococcal cutaneous infections. *J. Health Sci*., 54: 589-595.

Sargsyan, K., C. Grauffel and C. Lim. 2017. How molecular size impacts RMSD applications in molecular dynamics simulations. *J. Chem. Theory Comput.*, 13(4): pp. 1518-1524.

Sasidharan, S., Y. Chen, D. Saravanan, K.M. Sundram and L. Yoga-Latha. 2011. Extraction, isolation and characterization of bioactive compounds from plants extracts. *Afr. J. Trad. Complem. Alter. Med.*, 8: 1-9.

Zdenka, K., K. Kozics, Y. Bader, P. Saiko, N. Handler, T. Erker and T. Szekeres. 2006. Antioxidant activity of resveratrol, piceatannol and 3,3′,4,4′, 5,5′-hexahydroxy-trans-stilbenein three leukemia cell lines. *Oncol Rep*., 16:617–624.

Thuy, B.T.P., T.T.A. My, N.T.T Hai, L.T. Hieu, T.T. Hoa, H.T.P. Loan, N.T. Triet, T.T.V. Anh, P.T. Quy, P.V. Tat, N.V. Hue, D.T. Quang, N.T. Trung, V.T. Tung, L.K. Huynh and N.T.A. Nhung. 2020. Investigation into SARS-CoV-2 Resistance of compounds in garlic essential oil. *ACS Omega.*, 5: 8312-8320.

Tri, M.D., N.T. Phat, P.M.Nhat, M.T. Chi, B.X. Hao,T.N.M. An, M. Alam, N.V. Kieu, V.S. Dang, T.T.N. Mai and T.H. Duong. 2023. *In vitro* anti-inflammatory, *In silico* molecular docking and molecular dynamics simulation of oleanane-type triterpenes from aerial parts of *Mussaenda recurvata*. *RSC Adv*., 13: 5324-5336.

Vo, G.V., T.H.T. Nguyen, T.P. Nguyen, T.H.T. Do, N.M.A. Tran, H.T. Nguyen and T.T. Nguyen. 2022. *In silico* and *In vitro* studies on the anti-cancer activity of artemetin, vitexicarpin and penduletin compounds from *Vitex negundo*. *Saudi Pharm. J.*, 30: 1301-1314.

Trinh, P.T.N., T.N.M. An, T.T.Danh, H.A.N.Thi, V.K. Nguyen, T.H. Duong and L.T. Dung. 2023. The *In silico* and *In vitro* anti-inflammatory and antibacterial activities of flavonoids from *Artemisia vulgaris* in vietnam. *Curr Org Chem.*, 27: 1179-1190.

Van-Der-Spoel, D., E. Lindahl, B. Hess, G. Groenhof, A.E. Mark and H.J.C. Berendsen. 2005. GROMACS: Fast, flexible, and free. *J Comput. Chem*., 26: 1701-1718.

Xia, E.Q., B. Cui, X.R. Xu, Y. Song, X.X. Ai and H.B. Li. 2011. Microwave-assisted extraction of oxymatrine from sophora flavescens. *Molecules*, 16: 7391-7400.

Xu, D.P., J. Zheng, Y. Zhou, Y. Li, S. Li and H.B. Li. 2017. Ultrasound-assisted extraction of natural antioxidants from the flower of *Limonium sinuatum*: Optimization and comparison with conventional methods. *Food Chem.*, 217: 552-559.

(Received for publication 26 January 2024)